ISBN: 978-3-95450-227-1 ISSN: 2673-5490 doi:10.18429/JACoW-IPAC2022-TUPOMS012

INVESTIGATION OF SPECTRO-TEMPORAL PROPERTIES OF CHG RADIATION AT DELTA*

A. Radha Krishnan† , B. Büsing, A. Held, H. Kaiser, S. Khan, C. Mai, Z. Usfoor, V. Vijayan
Center for Synchrotron Radiation (DELTA), TU Dortmund, Dortmund, Germany

Abstract

At the synchrotron light source DELTA operated by the TU Dortmund University, the short-pulse facility employs the seeding scheme coherent harmonic generation (CHG) and provides ultrashort pulses in the vacuum ultraviolet and terahertz regime. Here, the interaction of laser pulses with the stored electron bunches results in a modulation of the longitudinal electron density which gives rise to coherent emission at harmonics of the laser wavelength. The spectral and temporal properties of such coherent short pulses can be manipulated by the seed laser and magnetic chicane properties. CHG spectra at several harmonics of the 800 nm seed laser were recorded using an image-intensified CCD (iCCD) camera and a newly installed XUV spectrometer. Numerical simulations to calculate the spectral phase properties of the seed laser from the observed spectra were carried out.

INTRODUCTION

Synchrotron radiation is a vital tool in studying the properties of matter in a variety of experiments, thanks to its characteristics such as high intensity, collimation and tunable wavelength. However, the minimum pulse length is limited by the electron bunch length which is in the order of several tens of picoseconds. These pulses lack the temporal resolution to probe the atomic processes taking place on the sub-picosecond scale. On the other hand, conventional mode-locked lasers can produce light pulses in the femtosecond regime but are usually of long-wavelengths. Coherent harmonic generation (CHG) [1] is a technique that combines the advantages of these two radiation sources to produce coherent femtosecond light pulses of short wavelength.

CHG is similar to the high-gain harmonic-generation seeding scheme used for free-electron lasers (FEL), but without the FEL gain in conventional storage rings [2–4]. As depicted in Fig. 1, CHG is based on a laser-electron interaction in an undulator that is tuned to the seed laser wavelength (modulator). This results in a sinusoidal modulation of the electron energy, which is transformed into a density modulation (microbunches) via a magnetic chicane. In a subsequent undulator (radiator), the microbunches produce coherent emission at harmonics of the laser wavelength. Since the laser pulse only modulates a very short slice of the electron bunch, the resulting coherently emitted pulse will also have a pulse length comparable to that of the laser pulse.

The power of the CHG radiation at the n^{th} harmonic of the laser wavelength λ is given by

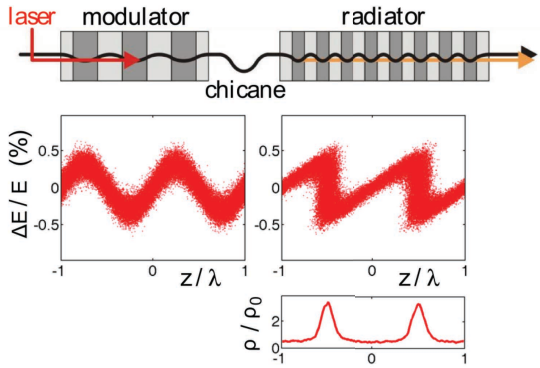

Figure 1: Magnetic setup for CHG, corresponding longitudinal phase space distributions and final longitudinal electron density.

$$P_n(\lambda) \sim N_e^2 b_n^2(\lambda) \tag{1}$$

where b_n is the bunching factor and N_e is the number of modulated electrons. For the CHG scheme, the bunching factor is given by [5],

$$b_n = |J_n(nAB)| e^{-\frac{n^2 B^2}{2}} \tag{2}$$

where $A = \Delta E_{\max}/\sigma_E$ is the relative energy modulation amplitude and $B = R_{56} k \sigma_E / E_0$ is the dimensionless chicane parameter. Here R_{56} is the matrix element of the chicane describing its longitudinal dispersion, E_0 is the nominal beam energy, σ_E is the rms energy spread and $k = 2\pi/\lambda$. When seeded with a laser pulse, the energy modulation amplitude A follows the pulse shape of the laser. Due to this non-uniform energy modulation, the chicane parameter influences the pulse shape of the CHG radiation. As can be seen in Fig. 2, at an R_{56} of 45 μm (green line) where the bunching is maximized, the resulting CHG radiation will be a single bell-shaped pulse. For stronger chicanes, e.g. 100 μm (red line), microbunching occurs for the electrons with a lower energy modulation at the head and tail of the modulated slice, while the electrons at the centre with maximum energy modulation are overbunched. Consequently, this results in separate pulses originating from different longitudinal positions. This allows one to manipulate the CHG pulse shape by tuning the laser and chicane properties, as demonstrated in the case for FERMI [6].

The spectral content of the CHG pulses does not only depend on R_{56}, but also on the wavelength distribution along the seed pulse. A laser pulse can be expressed in the frequency domain in terms of spectral amplitude $\tilde{E}(\omega)$ and spectral phase $\phi(\omega)$

* Work supported by BMBF (05K16PEA, 05K19PEB), DFG (INST 212/236-1 FUGG) and the federal state of NRW.
† arjun.krishnan@tu-dortmund.de

Content from this work may be used under the terms of the CC BY 4.0 licence (© 2022). Any distribution of this work must maintain attribution to the author(s), title of the work, publisher, and DOI

ISBN: 978-3-95450-227-1 ISSN: 2673-5490 doi:10.18429/JACoW-IPAC2022-TUPOMS012

Content from this work may be used under the terms of the CC BY 4.0 licence (© 2022). Any distribution of this work must maintain attribution to the author(s), title of the work, publisher, and DOI

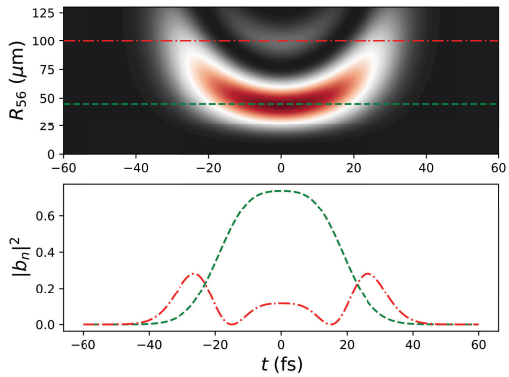

Figure 2: Intensity plot of theoretical bunching factor as a function of longitudinal position and chicane strength R_{56} (top). Bunching factor squared as a function of time along the specified lines in the top figure (bottom).

$$\tilde{E}(\omega) = |\tilde{E}_0(\omega)|e^{-i\phi(\omega)} \tag{3}$$

, where $\phi(\omega)$ can be expanded into a Taylor series as

$$\phi(\omega) = \phi(\omega_0) + \phi'(\omega_0).(\omega - \omega_0) + \frac{1}{2}\phi''(\omega_0).(\omega - \omega_0)^2 + \frac{1}{6}\phi'''(\omega_0).(\omega - \omega_0)^3 + \ldots \quad . \tag{4}$$

Here, the second-order term ϕ'', called group delay dispersion (GDD), introduces a linear frequency chirp to the laser pulse. If the seed pulse is not chirped the successive pulses have the same frequency which result in interference fringes in the CHG spectra at high R_{56} values as shown in Fig. 3 (left). Instead, if the seed pulse has strong frequency chirp, the successive maxima of the bunching factor would result in maxima at specific frequencies in the CHG spectra, see Fig. 3 (right)).

Studies exploring the spectral and temporal properties of the CHG radiation have been carried out previously at DELTA [7], but interpreting the spectra was difficult due to the higher-order dispersion present in the seed pulses. In this work, we attempted to include the effects of higher-order spectral phase on the spectral and temporal properties of the CHG radiation.

THE DELTA SHORT-PULSE SOURCE

At the university-based 1.5 GeV electron storage ring DELTA, a short-pulse facility based on the CHG scheme is being operated to produce ultrashort synchrotron radiation pulses in the vacuum ultraviolet wavelength regime [4]. Relevant parameters of the storage ring, the undulators and the laser system are given in Table 1.

Pulses from a titanium:sapphire laser system are focused directly through a beamline into the electromagnetic undulator U250 or are frequency-doubled first. The 7 upstream/downstream periods of the U250 act as modulator/radiator for CHG with a chicane between them. A diagnostics beamline is used to observe the spatial and temporal overlap of the laser pulse and the electron bunch with the help of screens and a streak camera. The laser-electron overlap is optimized by maximizing the intensity of THz radiation from a dipole magnet downstream.

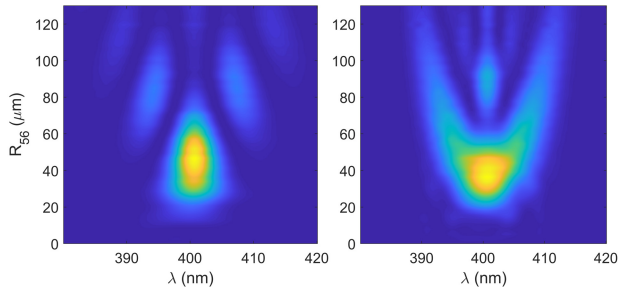

Figure 3: (Left) Simulated CHG spectra for a seed pulse with zero frequency chirp. (Right) Simulated spectra for a seed pulse with strong chirp.

Table 1: Parameters of the DELTA Short-pulse Facility

storage ring circumference	115.2 m
electron beam energy	1.5 GeV
beam current (single-/multibunch)	20/130 mA
horizontal emittance	15 nm rad
relative energy spread (rms)	7×10^{-4}
bunch length (FWHM)	80 ps
modulator/radiator period length	0.25 m
number of modulator/radiator periods	7
undulator periods used as chicane	3
max. modulator/radiator K parameter	10.5
max. chicane R_{56} (@ 800 A)	~ 170 μm
laser wavelength	800 nm
pulse energy @ 800 nm	8 mJ
min. pulse length	40 fs
repetition rate	1 kHz

OBSERVATION OF CHG SPECTRA

The spectra of the CHG radiation are recorded using a Czerny-Turner-type spectrometer equipped with an image-intensified CCD (iCCD) camera [8]. Wavelengths down to 190 nm can be recorded using this method, which covers the 2nd, 3rd and 4th harmonic of the seed wavelength. For observing even shorter wavelengths, a new XUV spectrometer was installed recently which can record spectra down to 30 nm [9]. Presently a MgF vacuum window blocks wavelengths below around 130 nm which needs to be removed to probe CHG radiation at higher harmonics. Nevertheless, with the current configuration, it is possible to record CHG spectra up to the 6th harmonic (133 nm) of the seed wavelength. Shown in Fig. 4 are the observed CHG spectra for the 2nd, 4th and 6th harmonic of the 800 nm seed without (left column) and with (right column) frequency chirp. It

ISBN: 978-3-95450-227-1 ISSN: 2673-5490 doi:10.18429/JACoW-IPAC2022-TUPOMS012

can be seen that when seeding with an unchirped laser pulse, pronounced spectral fringes appear at large R_{56} values as expected. On the other hand, seeding with a strongly chirped laser pulse results in a parabolic feature similar to the simulations. The asymmetry observed in the spectral features may be attributed to the higher-order dispersion in the seed laser pulse.

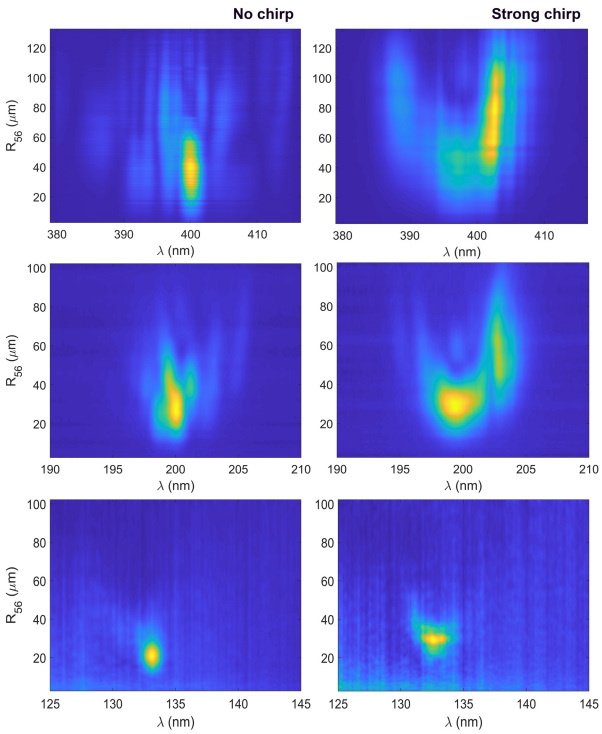

Figure 4: Observed CHG spectra for the 2nd, 4th and 6th harmonic of the seed laser wavelength with unchirped seed pulse (left) and with strong positive chirp (right).

COMPARISON WITH SIMULATIONS

The spectra of CHG radiation were simulated for seed laser pulses with various laser spectral phases. Emphasis was given to the effect of GDD and third-order dispersion (TOD) (ϕ''' in Eq. (4)) on the observed spectra. A convolutional neural network (CNN) [10] was designed using TensorFlow [11] to predict the GDD and TOD from the CHG spectra given as input. The CNN was trained on a set of over 4000 numerically simulated spectra for different combinations of GDD and TOD. Using the trained model, the GDD and TOD were predicted from spectra recorded for different spectral phases. The phase was controlled using an optical compressor based on a pair of gratings. Figure. 5 shows the observed and predicted spectra using the CNN for two different compressor settings.

The trained neural network could reconstruct the spectral features observed for different compressor settings by predicting the GDD and TOD of the seed laser pulse. A linear relationship between the distance between the gratings in the

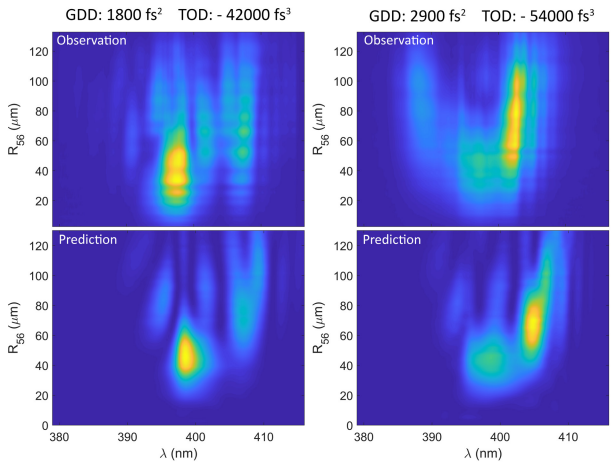

Figure 5: Observed and predicted CHG spectra for different settings of the laser compressor at the 2nd harmonic of the seed laser wavelength.

compressor and the GDD of the laser pulse was observed (Fig. 6 (left)), while there was no clear trend for the TOD in relation to the compressor length (Fig. 6 (right)). The results suggest that the asymmetry visible in the spectra could be due to a large negative TOD (> 40000 fs^3) present in the seed laser pulse because of the compressor under-compensating the TOD introduced by the pulse stretcher. A more detailed study using direct measurements of the spectral and temporal properties of the seed pulse, such as frequency resolved optical gating (FROG) [12], is required to confirm the effects of higher-order dispersion on the CHG spectra.

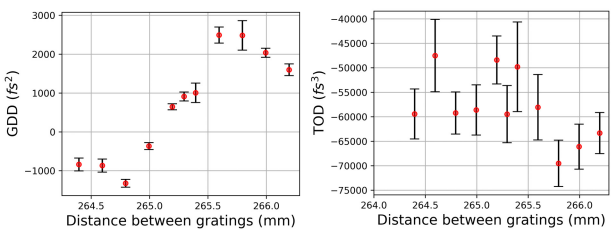

Figure 6: Predicted GDD and TOD values for different compressor settings. The error bars indicate the standard deviation of predictions from ten individually trained identical models.

ACKNOWLEDGEMENTS

We are pleased to thank our colleagues at DELTA and the TU Dortmund University. The continuous support from other institutes, particularly from DESY Hamburg, HZB Berlin, and KIT Karlsruhe is gratefully acknowledged.

REFERENCES

[1] R. Coisson and F. De Martini, "Free-electron coherent relativistic scatterer for UV-generation", *Physics of Quantum Electronics*, vol. 9, pp. 939–960, 1982.

Content from this work may be used under the terms of the CC BY 4.0 licence (© 2022). Any distribution of this work must maintain attribution to the author(s), title of the work, publisher, and DOI

ISBN: 978-3-95450-227-1 ISSN: 2673-5490 doi:10.18429/JACoW-IPAC2022-TUPOMS012

[2] M. Labat *et al.*, "Coherent harmonic generation on UVSOR-II storage ring", *Eur. Phys. J. D*, vol. 44, pp. 187–200, 2007. doi:10.1140/epjd/e2007-00177-6

[3] G. De Ninno *et al.*, "Generation of Ultrashort Coherent Vacuum Ultraviolet Pulses Using Electron Storage Rings: A New Bright Light Source for Experiments", *Phys. Rev. Lett.*, vol. 101, p. 053902, 2008. doi:10.1103/PhysRevLett.101.053902

[4] S. Khan *et al.*, "Generation of ultrashort and coherent synchrotron radiation pulses at DELTA", *Sync. Rad. News*, vol. 26, no. 3, pp. 25–29, 2013. doi:10.1080/08940886.2013.791213

[5] G. Stupakov, "Using the beam-echo effect for generation of short-wavelength radiation", *Phys. Rev. Lett.*, vol. 102, p. 074801, 2009. doi:10.1103/PhysRevLett.102.074801

[6] D. Gauthier *et al.*, "Spectrotemporal Shaping of Seeded Free-Electron Laser Pulses", *Phys. Rev. Lett.*, vol. 115, p. 114801, 2015. doi:10.1103/PhysRevLett.115.114801

[7] M. Huck *et al.*, "Ultrashort and Coherent Radiation for Pump-probe Experiments at the DELTA Storage Ring", in *Proc. IPAC'14*, Dresden, Germany, Jun. 2014, pp. 1848–1851. doi:10.18429/JACoW-IPAC2014-WEOAA03

[8] Andor iStar DH334T 18U-E3.

[9] HP Spectroscopy easyLIGHT XUV.

[10] Y. LeCun, Y. Bengio, and G. Hinton, "Deep learning", *Nature*, vol. 521, pp. 436–444, 2015. doi:10.1038/nature14539

[11] M. Abadi *et al.*, "Tensorflow: A system for large-scale machine learning", in *Proc. of 12th USENIX Symposium on Operating Systems Design and Implementation*, Savannah, GA, USA, Nov. 2016, pp. 265–283.

[12] R. Trebino *et al.*, "Measuring ultrashort laser pulses in the time-frequency domain using frequency-resolved optical gating", *Rev. Sci. Instrum.*, vol. 68, no. 9, p. 3277, 1997. doi:10.1063/1.1148286

Content from this work may be used under the terms of the CC BY 4.0 licence (© 2022). Any distribution of this work must maintain attribution to the author(s), title of the work, publisher, and DOI